THE JOURNAL OF PHYSICAL CHEMISTRY B

Article

pubs.acs.org/JPCB

Diffusion–Viscosity Decoupling in Solute Rotation and Solvent Relaxation of Coumarin153 in Ionic Liquids Containing Fluoroalkylphosphate (FAP) Anion: A Thermophysical and Photophysical Study

Sudhir Kumar Das, Prabhat Kumar Sahu, and Moloy Sarkar*

School of Chemical Sciences, National Institute of Science Education and Research, Bhubaneswar 751005, India

Supporting Information

ABSTRACT: Steady state and time-resolved fluorescence behavior of coumarin153 (C153) has been investigated in two ionic liquids (ILs), namely 1-(2-methoxyethyl)-1-methylpyrrolidinium tris(pentafluoroethyl)trifluorophosphate ([MOEMPL][FAP]) and 1-(2-methoxyethyl)-1-methylmorpholinium tris(pentafluoroethyl)trifluorophosphate ([MOEMMO][FAP]) in order to find out the viscosity–diffusion decoupling during solvation and rotational relaxation of C153. Thermophysical studies have also been carried out to understand the physicochemical properties of the media. At 293 K, the measured viscosity of [MOEMMO][FAP] is 8 times higher than that of [MOEMPL][FAP]. The data obtained from steady state and time-resolved fluorescence measurements show the deviation of average solvation and rotation times from conventional hydrodynamics. The decoupling of solute and solvent dynamics from medium viscosity is manifested through fractional viscosity dependence (η) of the measured average solvation ($\langle\tau_s\rangle$) and rotation ($\langle\tau_r\rangle$) times: $\langle\tau_x\rangle \propto (\eta/T)^p$ (x denotes solvation or rotation and T is the temperature) covering the p value $0.69 < p < 0.85$ for solvent relaxation and $0.48 < p < 1.10$ for solute rotation. The excitation wavelength dependent fluorescence studies have been performed to correlate the experimental findings with the heterogeneity of the medium. While the excitation wavelength dependent time-resolved fluorescence studies of coumarin153 reveal a very similar variation of average solvation time with a change in excitation wavelengths for both the ionic liquids, the steady state excitation wavelength dependent measurements of 2-amino-7-nitrofluorene (ANF) show a higher (630 cm^{-1}) shift of the fluorescence maximum for highly viscous ionic liquid as compared to that (430 cm^{-1}) of another much less viscous ionic liquid. The recent theoretical (*Chem. Phys. Lett.* **2011**, *517*, 180) and experimental (*J. Chem. Phys.* **2012**, *136*, 174503) findings and the outcome of the excitation wavelength dependent fluorescence measurements in the present case seem to suggest that both static and dynamic heterogeneity may play an important role in the observed viscosity–diffusion (d–η) decoupling for highly viscous ionic liquid.

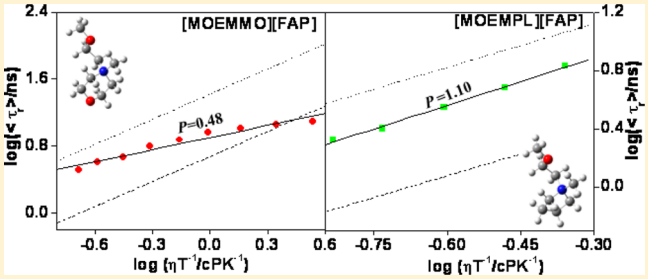

1. INTRODUCTION

In recent years the intense interest in room temperature ionic liquids (RTILs) is primarily because of two broad reasons: (i) their potential as a specialty media for advanced devices and industrial processes[1] and (ii) scientific curiosity to unravel their structure–property correlation.[2] However, molecular-level understanding of the intermolecular interactions, structure, and dynamics of new solvent systems is very much essential for that substance to be used in new applications. Since solvation dynamics, the time dependent response of solvent molecules to an electronic redistribution in solute molecules,[3] is intricately related to the rate of chemical reactions, considerable attention has been paid to understand this phenomenon in this specialized solvent sytems.[4−10] The dynamics of solvation in ionic liquid is found to be quite complex.[4h] It is not yet possible to quantitatively describe the connection between dynamics and structures of RTILs. In this regard, microheterogeneous nature of ILs has made it even more challenging to find out the structure–property correlation. So, the studies that focus unraveling the relationship between microheterogeneous nature of RTILs and the dynamical feature of RTILs are the need of the hour.

A limited number of studies have been performed on ionic liquids to understand the microheterogeneous nature of RTILs.[11] The multiscale coarse grained structure simulation by Wang and Voth[11a] and atomistic simulations by Lopes and Padua[11b] indicated nanostructural organization in these media. Recently, optical heterodyne-detected Raman induced Kerr effect studies (OHD-RIKES) provide further evidence in favor of heterogeneous nature of ILs.[11c] Samanta and co-workers have also shown the microheterogeneous nature of ionic liquids by exploiting excitation wavelength dependence fluorescence

Received: October 12, 2012
Revised: November 27, 2012
Published: December 20, 2012

behavior of several probes in RTILs.[11d] Later, Hu and Margulis[11h] by molecular dynamics simulation studies proposed that the red edge excitation wavelength fluorescence behavior of molecules arises from probes trapped in quasistatic solvent cages that relax on a time scale longer than the fluorescence lifetime of the probes. Very recently, Maroncelli[11k] and Bhattacharya and co-workers[11n] have studied the excitation wavelength dependent solvation dynamics in neat ionic liquids using femtosecond time-resolved emission spectroscopy. In this context, recent time-resolved fluorescence studies by Biswas and co-workers in deep eutectic mixtures containing amide and electrolytes are noteworthy.[12a−d] They have observed the decoupling of solute rotation and solvation dynamics from the medium viscosity. They have also shown that medium heterogeneity plays an important role for this observed behavior. Deep eutectic melts consist of amide and electrolytes (a system that contains the same pieces of solvent−solvent interactions as these ionic liquids and thus understanding gained there may be utilized to explain some of the results obtained in the present study). It may be mentioned that the viscosity−diffusion decoupling has been commonly analyzed by fractional viscosity dependence (η) of the measured average solvation $\langle\tau_s\rangle$ and rotation $\langle\tau_r\rangle$ times: $\langle\tau_x\rangle \propto (\eta/T)^p$ (x denotes solvation or rotation, p is the exponent, and T is the temperature).[12a−d] Since the ILs and eutectic melts are very similar in nature; we are interested to know whether such fractional dependence of viscosity is also observed in the case of average solvation and rotational times in ILs. Additionally, we are interested to know the roles of both static and dynamic heterogeneities that play in governing the viscosity decoupling in these media. In this regard, it may be mentioned that the studies on eutectic melts are mostly based on single excitation wavelength based measurements and hence cannot provide much insights into the temporal heterogeneity of the medium. To the best of our knowledge no such studies that focus on investigating the role of static and dynamic heterogeneity in the observed viscosity−diffusion decoupling for room temperature ionic liquids have been carried out.

Keeping all these aspects in mind, we have carried out the temperature as well as excitation wavelength dependence solvation and rotational relaxation of C153 in 1-(2-methoxyethyl)-1-methylpyrrolidinium tris(pentafluoroethyl)-trifluorophosphate ([MOEMPL][FAP]) and 1-(2-methoxyethyl)-1-methylmorpholinium tris(pentafluoroethyl)-trifluorophosphate ([MOEMMO][FAP]). Thermophysical properties of the two ionic liquids have also been investigated with a view to understand how the structural variation in the cationic moiety affects the properties of the ionic liquids. Structural information of the ILs and C153 is provided in Chart 1. The choice of ILs is primarily governed by the fact that the moisture and halide contents of these ILs are very low (water and halides both less than 100 ppm) .[13] We have chosen C153 as the fluorescence probe due to its suitable photophysical properties.[14]

2. EXPERIMENTAL SECTION

2.1. Materials. Coumarin153 (C153) (laser grade, Exciton) was used as received. RTILs (Chart 1) were obtained from Merck, Germany (>99% purity), and used as received. The water and halide contents of the ILs were <100 ppm. The RTILs were transferred into a different long-necked quartz cuvette, and the requisite amount of C153 was added to prepare the solution taking precaution to avoid moisture absorption by this media. The long-necked quartz cuvette was sealed with septum and parafilm to further ensure dry condition.

Chart 1. Structures of the RTILs and Coumarin153 (C153)

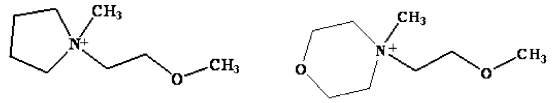

1-(2-methoxyethyl)-1-methylpyrrolidinium [MOEMPL]

N-(2-methoxyethyl)-*N*-methylmorpholinium [MOEMMO]

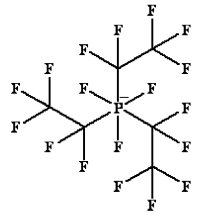

tris(pentafluoroethyl)trifluorophosphate [FAP]

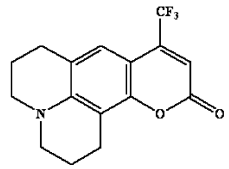

Coumarin153 (C153)

2.2. Instrumentation. The absorption and fluorescence spectra were measured using Perkin-Elmer (Lambda-750) spectrophotometer and Perkin-Elmer LS 55 spectrofluorimeter, respectively. The fluorescence spectra were corrected for the spectral sensitivity of the instrument. For steady-state experiments, all samples were excited at 375, 405, and 445 nm, respectively. Time-resolved fluorescence measurements were carried out using a time-correlated single-photon counting (TCSPC) spectrometer (Edinburgh, OB920). The samples were excited at 375, 405, and 445 nm using different picoseconds laser diode (EPL), and the signals were collected at magic angle (54.7°) using a Hamamatsu microchannel plate photomultiplier tube (R3809U-50). The lamp profile was recorded by scatterer (dilute Ludox solution in water) in place of the sample. The instrument response functions (fwhm) of our setup were ∼75 ps for 375 nm, 95 ps for 405 and 445 nm picoseconds diode laser, respectively. Decay curves were analyzed by nonlinear least-squares iteration procedure using F900 decay analysis software. The qualities of the fit were judged by the chi square (χ^2) values, and weighted deviations were obtained by fitting. The same setup was used for anisotropy measurements. The emission intensities at parallel ($I_\parallel$) and perpendicular ($I_\perp$) polarizations were collected alternatively until peak difference between parallel ($I_\parallel$) and perpendicular ($I_\perp$) decay (at t = 0) ∼5000 was reached. For G-factor calculation, the same procedure was adopted, but with 5 cycles and horizontal polarization of the exciting laser beam. The same software was also used to analyze the anisotropy data. The temperature was maintained by circulating water through the cell holder using a Quantum, North West (TC 125) temperature controller. The viscosities of the RTIL were measured by LVDV-III Ultra Brookfield Cone and Plate viscometer (1% accuracy and 0.2% repeatability), and densities were measured at different temperatures using density meter (Anton Parr, DMA 5000).

2.3. Method. The time-resolved decay profiles were measured at 5/10 nm intervals across the entire steady-state emission spectra at magic angle (54.7°). The total numbers of measurements were 30−35 in each case. For deconvoluting the instrument response function, each decay curve was fitted by

dx.doi.org/10.1021/jp3101199 | J. Phys. Chem. B 2013, 117, 636−647

using a triexponential decay function to obtain a χ^2 value between 1 and 1.2 which indicated the goodness of fit. The collected intensity decays at magic angle had been analyzed using a standard method.[15] The peak frequencies obtained from the log-normal fitting of time-resolved emission spectra (TRES) were then used to construct the decay of solvent correlation function ($C(t)$) which is given below.

$$C(t) = \frac{\bar{\nu}(t) - \bar{\nu}(\infty)}{\bar{\nu}(0) - \bar{\nu}(\infty)} \quad (1)$$

Here $\bar{\nu}(\infty)$, $\bar{\nu}(0)$, and $\bar{\nu}(t)$ are the peak frequencies at times infinity (∞), zero ($t = 0$), and t, respectively. The time dependence of the calculated $C(t)$ was fitted by a biexponential function as given below

$$C(t) = a_1 e^{-t/\tau_1} + a_2 e^{-t/\tau_2} \quad (2)$$

where τ_1 and τ_2 are the solvent relaxation time and a_1 and a_2 are normalized preexponential factors. After having the value of τ_1, τ_2, a_1, and a_2, the average solvation times were calculated by using the relation

$$\langle \tau_{av} \rangle = a_1\tau_2 + a_2\tau_2 \quad (3)$$

We had also fitted $C(t)$ by the stretched exponential function shown below.

$$C(t) = \exp(-(t/\tau_{solv})^{\beta}) \quad (4)$$

If $0 < \beta \leq 1$

$$\langle \tau_{st} \rangle = \frac{\tau_{solv}}{\beta}\Gamma(\beta^{-1}) \quad (5)$$

where Γ was gamma function and τ_{st} was the average solvation time considering $C(t)$ was a stretched exponential function.

3. RESULTS AND DISCUSSION

3.1. Thermophysical Properties of RTILs. The properties of the RTILs depend very much on the cations and anions that they are composed of and for that they are also known as designer solvents.[2] In order to know the effects of cationic moiety in controlling the physicochemical properties of the ionic liquids, thermophysical studies on the present ionic liquids that differ only in their cationic moiety have been carried out. The knowledge about the physicochemical properties of the ILs is also expected to be helpful in explaining the new experimental observation such as photophysical responses of the systems in proper manner. The measured viscosity and density of the two ionic liquids at different temperatures are provided in the Supporting Information (Table S1). The variations of the viscosity and density of the two ionic liquids at different temperatures are also shown in Figures 1 and 2. It is evident that, at 293 K, viscosity of morpholinium-based system is almost 8 times higher than that of pyrolidinium-based system. This difference in viscosity may be due to the presence of oxygen atom in the ring which renders the nitrogen atom more electropositive by virtue of the greater inductive effect of oxygen than carbon atom, which in turn makes the association with the FAP anion stronger.[10c] The fact that N atom of morpholinuim cation is more electropositive than the N atom of pyrrolidinum moiety is supported by calculation of charge densities on the N atom by optimizing (at AM1level[16]) the structures (Figure 3) of two cations independently. All the calculations were performed using the

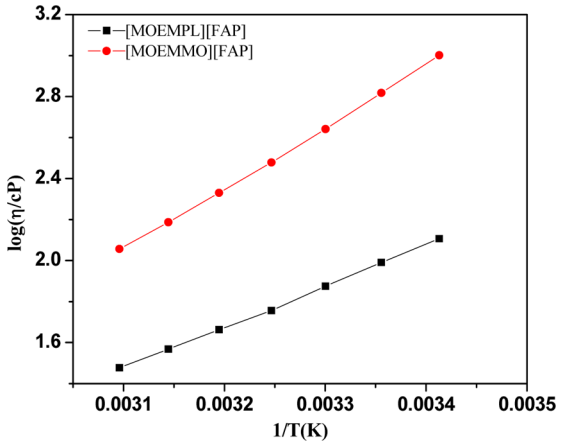

Figure 1. Viscosity as a function of temperature for [MOEMMO][FAP] and [MOEMPL][FAP].

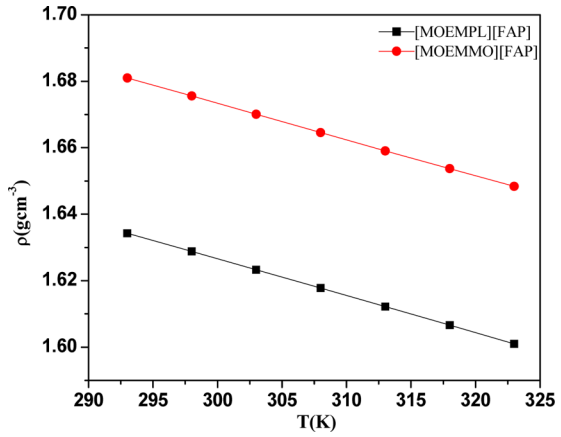

Figure 2. Densities as a function of temperature for [MOEMMO][FAP] and [MOEMPL][FAP].

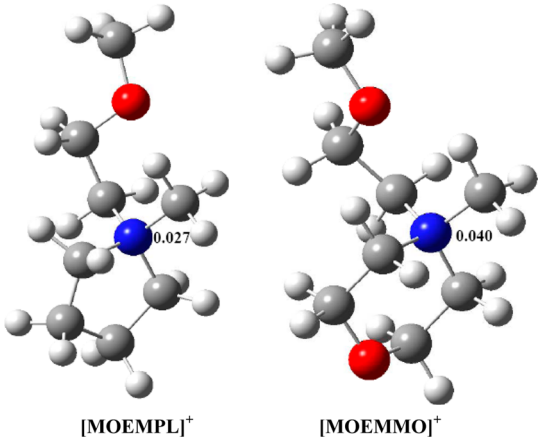

Figure 3. Optimized stricture of $[MOEMPL]^+$ and $[MOEMMO]^+$ at AM1 level theory.

GAUSSIAN 03 program package.[17] It is evident from Figure 1 that at all temperatures the viscosity of morpholinium-based system is always higher by a factor of 4−8 as compared to pyrrolidinium −based system.

The observation indicates that the association between cationic moiety and FAP anion always remains stronger even at higher temperature (323 K) for [MOEMMO][FAP] than for [MOEMPL][FAP]. It is also revealed from Figure 2 that at all

dx.doi.org/10.1021/jp3101199 | J. Phys. Chem. B 2013, 117, 636−647

temperatures the measured densities are slightly higher for [MOEMMO][FAP] than for [MOEMPL][FAP].

The experimental viscosity (η) and density (ρ) at different temperatures were fitted by the least-squares method using the following reported equations.[18,19]

$$\log \eta/cP = A_0 + (A_1/T) \quad (6)$$

$$\rho/(\mathrm{g\ cm^{-3}}) = A_2 + A_3 T \quad (7)$$

The values of A_0, A_1, A_2, A_3, and the correlation coefficients, are collected in Table 1.

Table 1. Fitting Parameters for Viscosity and Density According to Equations 6 and 7

RTILs	A_0	A_1	R	A_2	$A_3 \times 10^{-3}$	R^a
[MOEMMO][FAP]	−7.17	2975.72	0.9988	2.00	−1.09	0.9999
[MOEMPL][FAP]	−4.69	1991.15	0.9989	1.96	−1.11	0.9999

[a] R = regression coefficient.

The experimental density values were again used to estimate thermal expansion coefficient (α) of the two ILs by using the following equation[18]

$$\alpha_p = -\frac{1}{p}\left(\frac{\delta p}{\delta T}\right)_p = -\frac{A_3}{A_2 + A_3 T} \quad (8)$$

where A_2, A_3 are the fitting parameters from eq 7, and α_p, p, and T are the thermal expansion coefficient, pressure, and absolute temperature, respectively. It may be mentioned that the thermal expansion coefficient (α_p) is also known as volume expansivity.[20] The expansion coefficients of the two ionic liquids are collected in Table 2. It can be observed (see Table 2) that the coefficients of thermal expansion of the ionic liquids do not change appreciably with a change in temperature. The observed thermal expansion coefficient values are found to be similar to those reported for imidazolium, pyridinium, phosphonium, and ammonium based ILs (4.8×10^{-4} to 6.5×10^{-4}) K^{-1}.[21,22]

Table 2. Thermal Expansion Coefficients of the Ionic Liquids as a Function of Temperature

	$\alpha \times 10^4$ (K^{-1})[a]	
T/K	[MOEMPL][FAP]	[MOEMMO][FAP]
293	6.79	6.48
298	6.81	6.51
303	6.84	6.53
308	6.86	6.55
313	6.88	6.57
318	6.91	6.59
323	6.93	6.61

[a] Thermal expansion coefficients (α) using eq 8.

3.2. Steady State Behavior of C153 in RTILs. The representative absorption spectra of C153 in [MOEMPIL]-[FAP] and [MOEMMO][FAP] are shown in Figure 4. The emission spectra of neat RTILs and C153 in two RTILs at different excitation wavelength are shown in Figure 5. Absorption and emission maxima of C153 in [MOEMPIL]-[FAP] and [MOEMMO][FAP] are collected in Table 3. A bathochromic shift in both absorption and emission maxima of C153 has been observed on changing the medium from pyrrolinidium to morpholinium systems (Table 3). Addition-

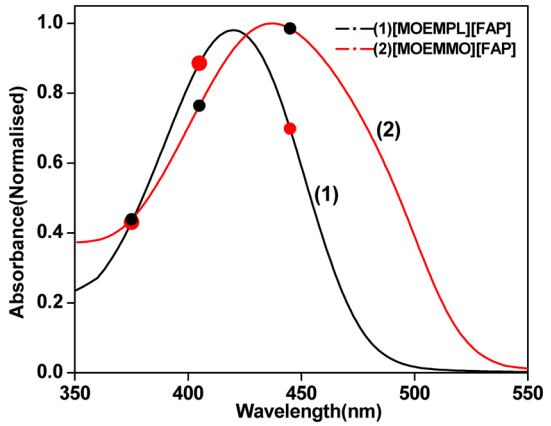

Figure 4. Steady state absorption spectra of C153 in [MOEMPIL]-[FAP] and [MOEMMO][FAP]. Spectra are normalized at the corresponding peak maximum. Symbols denote the excitation wavelengths (λ_{exc}).

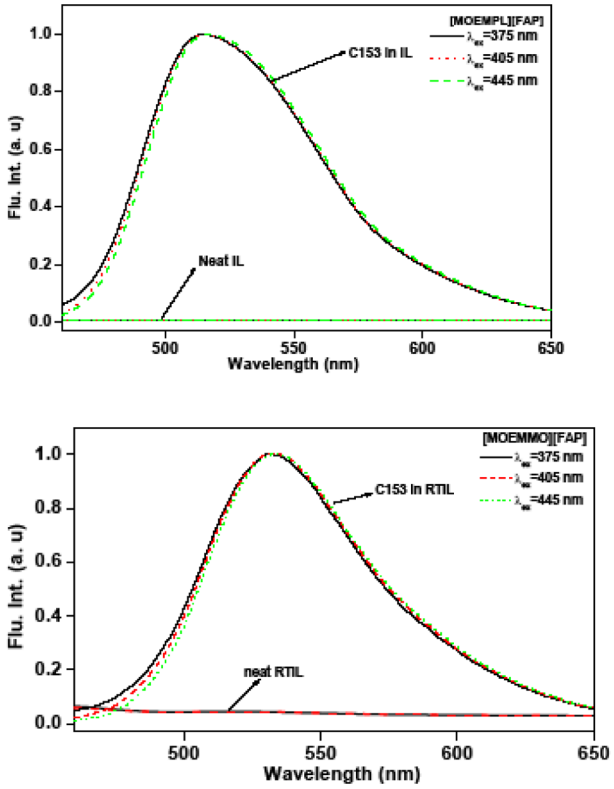

Figure 5. Steady state emission spectra of C153 in [MOEMPIL]-[FAP] and [MOEMMO][FAP] at different excitation wavelength (λ_{exc}) at 293 K. All emission spectra of C153 are normalized at the corresponding peak. Emission spectra of neat RTILs are also shown in corresponding figure at the different excitation wavelength (λ_{exc}).

Table 3. Absorption and Emission Maxima and Stokes' Shift of C153 in [MOEMPL][FAP] and [MOEMMO][FAP]

system	λ_{max}^{abs} (nm)	λ_{max}^{flu} (nm)	Stokes' shift (cm^{-1})
[MOEMPL][FAP]	420	515	4392
[MOEMMO][FAP]	437	533	4122

dx.doi.org/10.1021/jp3101199 | J. Phys. Chem. B 2013, 117, 636−647

ally, one can also observe from Figure 5 that the emission maxima of C153 in neat RTILs do not change with the variation of excitation wavelengths (λ_{exc}). No significant changes in both absorption and emission maximum of C153 have been observed with the change in temperature (293 K to 308 K). From the steady state absorption and emission spectral profile, it can be concluded that [MOEMMO][FAP] IL is more polar in nature than [MOEMPIL][FAP]. Interestingly, the full width at half-maximum (fwhm) as estimated from the absorption spectrum of C153 is found to be higher (5850 cm^{-1}) in [MOEMMO][FAP] than that (4360 cm^{-1}) in [MOEMPL][FAP]. The observation indicates a distribution of the molecules in the ground state having multiple solvation sites, and hence different energies. The more inhomogeneous broadening of absorption in the case of highly viscous ionic liquid points out that the presence of an ensemble of energetically different species in the ground state is more favored in a highly viscous medium. To know how the spectral widths (absorption and emission) of C153 in these ILs compare with those from imidazolium IL, we have also measured the fwhm of both the absorption and emission spectra in imidazolium-based ionic liquid, 1-ethyl-3-methyl-imidazolium tris(pentafluoroethyl)trifluorophosphate (EMIM-FAP). In the case of absorption, the measured fwhm in EMIMFAP is 4131 cm^{-1}. In the case of emission, the fwhm is measured to be 2803, 2395, and 2678 cm^{-1} for MOEMPLFAP, MOEMMOFAP, and EMIMFAP, respectively. These data probably indicate that morpholinium ILs are more micro-heterogeneous in nature than the imidazolium-based ILs. In this context we would like to note that a very recent work by Samanta and his co-workers has also pointed out that the morpholinium ILs are more heterogeneous in nature than imidazolium ILs.[4i]

3.3. Solvation Dynamics Study. As stated in the Experimental Section, the magic angle fluorescence decays of C153 are collected at 5/10 nm wavelength intervals covering the entire emission spectra. Wavelength-dependent decay profiles, which demonstrate the typical signature of slow solvation dynamics, have been observed in the present study. A representative wavelength dependent decay profile is given in Figure 6 for [MOEMMO][FAP] at λ_{exc} = 405 nm. When

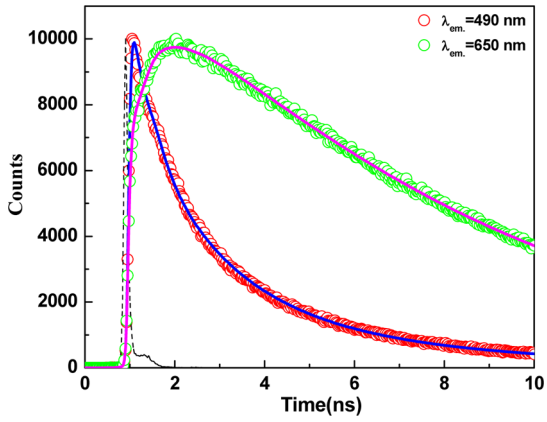

Figure 6. Representative emission wavelength dependent decay profile for C153 in [MOEMMO][FAP] at 293 K (λ_{exc} = 405 nm). Circles denote the experimental data points, and the solid lines represent the fit to the data points. Instrument response function (IRF) is also shown in the same figure (dotted lines). The goodness of fit parameters (χ^2) in these two wavelengths are1.1 and 1.01, respectively.

emissions are monitored at the shorter wavelength regions, only faster decay is observed, and at the longer wavelengths, the decay profiles consist of a slow rise followed by the decay. The time-resolved emission spectra (TRES) of C153 in [MOEMPL][FAP] at different time intervals are shown in Figure 7. A time-dependent shift of the emission spectra toward

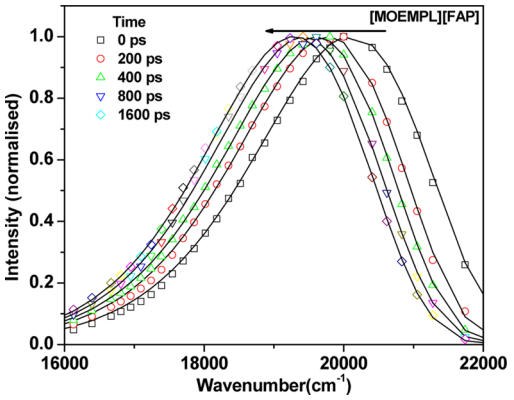

Figure 7. TRES of C153 in [MOEMPL][FAP] at 293 K at different time span at λ_{ex} = 405 nm. The time intervals are indicated by the corresponding symbols. All spectra are normalized at their corresponding peak maxima.

the lower energy indicates solvent-mediated relaxation of the excited state of the fluorophore (Figure 7). It is pertinent to mention in this context that the spectral widths (fwhm) of the TRES are becoming narrower with time which also indicates the solvent mediated stabilization of the excited state of the probe (see Supporting Information, Figure S1).[15] The total shift of time-dependent emission ($\Delta\bar{\nu}$), calculated from the difference between the peak frequencies (in cm^{-1}) of the measured spectra at zero time ($\bar{\nu}$ (0)) and infinite time ($\bar{\nu}$ (∞)), is found to be 924 and 479 cm^{-1} for C153 at λ_{ex} = 405 nm in [MOEMPL][FAP] and [MOEMMO][FAP], respectively (Table 4). These data indicate that ~30% dynamics is missed in the case of [MOEMPL][FAP] due to the finite time resolution of our TCSPC setup.[23] The missing component for highly viscous IL by employing the Fee and Maroncelli method[23] is found to be higher. The higher missing component in the case of a highly viscous ionic liquid is probably due to the underlying change in the vibronic structure of the solute.

The representative plots of $C(t)$ versus time for C153 both via biexponential and stretched exponential fit to the data are shown in Figure 8. Both fits are suitable as both fits provide very similar average solvation times (Tables 4–6). A representative plot which shows both biexponential and stretched exponential fitting is shown in the Supporting Information (Figure S2). The average solvation times are estimated to be different for different RTILs (Table 4) and also found to depend on the excitation wavelengths. For example, the average solvation times are estimated to be 0.61 and 3.10 ns at λ_{exc} = 375 nm and 0.69 and 3.65 ns at λ_{exc} = 405 nm in the case of [MOEMPL][FAP] and [MOEMMO][FAP], respectively (Table 4). Quite interestingly the data that are collected in Table 4 also reveal that even if the average solvation time is found to be much higher for morpholinium based ionic liquid compared to that of pyrrolidinium based system, the change in the average solvation time with respect to the change in the excitation wavelengths is quite similar. On changing the excitation wavelength from 375 to 405 nm, the change in the

dx.doi.org/10.1021/jp3101199 | J. Phys. Chem. B 2013, 117, 636–647

Table 4. Solvent Relaxation Parameters of C153 in [MOEMPL][FAP] and [MOEMMO][FAP] at Different Excitation Wavelengths

		from biexponential fit[a]						stretched exponential fit[b]			
RTIL	viscosity (cP)	λ_{ex} (nm)	a_1	τ_1 (ns)	a_2	τ_2 (ns)	$\langle\tau_s\rangle$ (ns)	β	τ_0	$\langle\tau_{st}\rangle$ (ns)	obsd shift (cm^{-1})
MOEMPLFAP	128	375	0.44	1.19	0.56	0.15	0.61	0.59	0.39	0.60	808
		405	0.46	1.18	0.54	0.27	0.69	0.76	0.56	0.66	924
		445	0.44	1.21	0.56	0.20	0.64	0.68	0.46	0.60	911
MOEMMOFAP	1004	375	0.47	5.85	0.53	0.67	3.10	0.63	2.18	3.08	483
		405	0.51	6.46	0.49	0.73	3.65	0.64	2.64	3.67	479

[a]Biexponential fit according to eq 3. [b]Stretched exponential fit according to eq 5. Experimental error ±5%

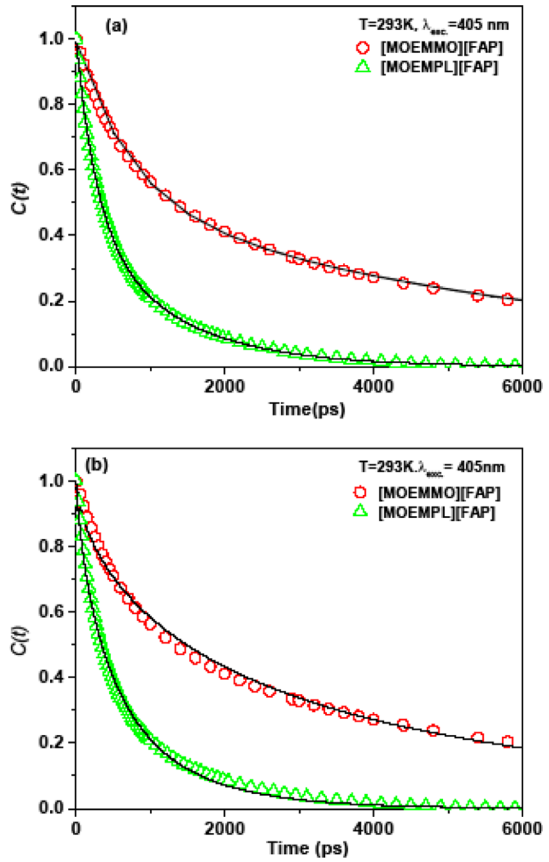

Figure 8. (a) Biexponential fits and (b) stretched exponential fits to spectral correlation function, $C(t)$, versus time plot of C153 in [MOEMPL][FAP] and [MOEMMO][FAP] at 293 K at λ_{ex} = 405 nm. Symbols are denoting the data points, and solid lines represent the corresponding fit to the data points.

average solvation time is found to be 1.13 and 1.17 times for pyrrolidinium and morpholinium based system, respectively. Quite interestingly, data in Table 4 also show that measured average solvation time exhibits stronger excitation wavelength dependence in highly viscous IL, whereas similar sensitivity has not been found in low viscous IL. For low viscous IL, the difference is negligible probably because of rapid interconversion (low lifetime compared to diffusive time scale of the medium) of the environments probed by the photoselection; at larger viscosity these distinct environments are relatively longer-lived, and thus, the measured average solvation time exhibits stronger excitation wavelength dependence. However, absence of the initial fast component in the present experiments may also have some effects on the observed dependence here which cannot be quantified by the present data. The change in average solvation times as a function of excitation wavelengths reflects the microheterogeneous nature of the RTILs. In this context we note that the excitation wavelength dependency on solvation dynamics has also been observed by Das et al.,[9c] Bhattacharyya and co-workers,[11m] and Maroncelli and co-workers[11k] independently in different ionic liquids, and the same rationale has been put forward in explaining the observation of excitation wavelength dependence solvation dynamics.

Quite interestingly, although the viscosity of [MOEMMO][FAP] is almost 8 times higher than that of [MOEMPL][FAP], solvation time is increased only 5.3 times at a particular wavelength (see Figure 9). Here it may be mentioned that average solvation time relates linearly with the viscosity[4h] of the medium, and hence, the present solvation dynamics data in the case of highly viscous IL is interesting. To get a better understanding of the coupling between average solvation time ($\langle\tau_s\rangle$) and medium viscosity (η), we have applied the Stokes–Einstein relation (SE) which predicts $D^{-1} \propto \eta/T$ where D is the diffusion coefficient and η/T is temperature-reduced viscosity. The similar relationship has also been applied by other authors in eutectic melts for the same purpose.[12d] We have fitted the average solvent relaxation time with the $\langle\tau_s\rangle \propto (\eta/T)^p$ relationship (eqs 9 and 10). In both the cases p is found to deviate from unity, and deviation is greater in the case of a relatively more viscous ionic liquid. However, in both cases the fractional dependence of average solvation time on temperature-reduced viscosity is not large, but not negligible. These findings are interesting in a sense that dynamic Stokes shift

Table 5. Solvent Relaxation Parameters of C153 in [MOEMMO][FAP] as a Function of Temperature and at λ_{ex} = 405 nm

		biexponential fit[a]					stretched[b] exponential fit			
temp (K)	viscosity (cP)	a_1	τ_1 (ns)	a_2	τ_2 (ns)	τ_{av}(ns)	β	τ_{solv} (ns)	τ_{st} (ns)	obsd shift (cm^{-1})
293	1004	0.51	6.46	0.49	0.73	3.65	0.64	2.64	3.67	479
298	657	0.54	3.75	0.44	0.51	2.25	0.68	1.77	2.30	498
303	438	0.51	3.04	0.49	0.49	1.79	0.70	1.39	1.76	508
308	301	0.57	2.38	0.43	0.35	1.51	0.69	1.19	1.63	613

[a]Biexponential fit according to eq 3. [b]Stretched exponential fit according to eq 5. Experimental error ±5%.

dx.doi.org/10.1021/jp3101199 | J. Phys. Chem. B 2013, 117, 636–647

Table 6. Solvent Relaxation Parameters of C153 in [MOEMPL][FAP] RTIL as a Function of Temperature and at λ_{ex} = 405 nm

		biexponential fit[a]					stretched exponential fit[b]			
temp (K)	viscosity (cP)	a_1	τ_1 (ns)	a_2	τ_2 (ns)	τ_{av} (ns)	β	τ_{solv} (ns)	τ_{st} (ns)	obsd shift (cm^{-1})
293	128	0.46	1.18	0.54	0.27	0.69	0.76	0.56	0.66	808
298	98	0.50	0.89	0.50	0.24	0.56	0.79	0.48	0.55	913
303	75	0.48	0.71	0.52	0.22	0.45	0.83	0.40	0.44	882
308	57	0.63	0.47	0.37	0.10	0.33	0.78	0.29	0.33	933

[a]Biexponential fit according to eq 3. [b]Stretched exponential fit according to eq 5. Experimental error ±5%.

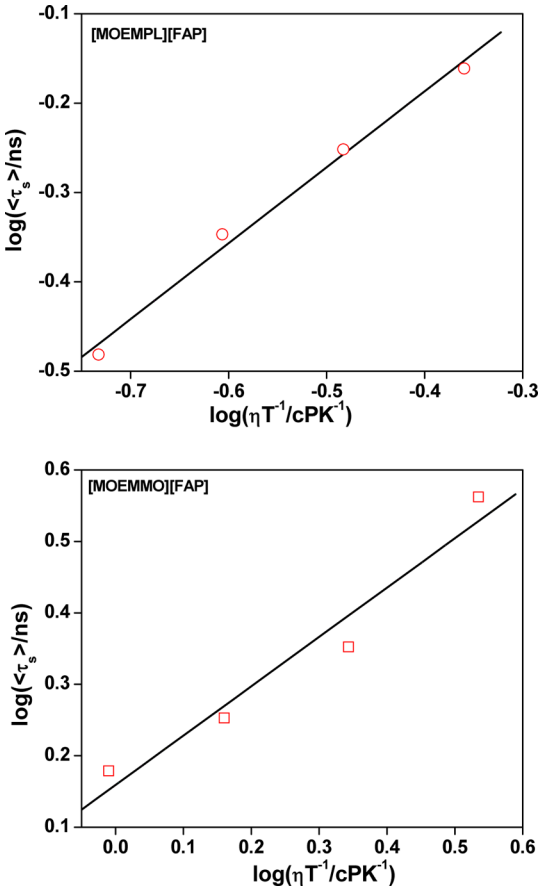

Figure 9. log–log plots of average solvent relaxation time ($\langle\tau_s\rangle$) of C153 vs η/T in [MOEMPL][FAP] and [MOEMMO][FAP]. Symbols denote experimental data points, and solid lines are linear fits to the data.

measurements in ionic liquids showed better linear correlation with viscosity.[24]

$$\text{C153 in [MOEMMO][FAP]}\ \log(\langle\tau_s\rangle) = 0.159 + 0.69\log(\eta/T)\ (N = 4,\ R = 0.97512) \quad (9)$$

$$\text{C153 in [MOEMPL][FAP]}\ \log(\langle\tau_s\rangle) = 0.153 + 0.85\log(\eta/T)\ (N = 4,\ R = 0.99568) \quad (10)$$

It is pertinent to mention here that very recently Biswas and co-workers[12d] have also observed fractional dependence of average solvation times on viscosity while studying Stokes shift dynamics in eutectic melts. However, they have observed a great degree of nonlinearity in SE relation. The present behavior has been attributed to the presence of pronounced heterogeneity in the medium.[12c,d] The mismatch between the predicted and measured solvation time constants has also been explained by them by following the same argument.[12d]The above-mentioned results led us to believe that the relatively poorer agreement between the measured average solvation time and expected solvation time in case of more viscous ionic liquid is perhaps due to the presence of strong heterogeneity of the medium which leads to the substantial decoupling of average solvation time with medium viscosity. It may be mentioned here that the fractional viscosity dependence of average solvation time that are observed in eutectic melts is similar to the observed viscosity decoupling of diffusion in deeply supercooled liquids,[25] and therefore, it was argued that possibly both static and dynamic heterogeneities in these melts may play an important role toward viscosity decoupling of diffusion.[12d] The heterogeneity aspect of these RTILs is further investigated by following the excitation wavelength (λ_{exc}) dependence of the steady state fluorescence emission by employing 2-amino-7-nitrofluorene (ANF) which has excited state lifetime (τ) ~100 ps[11d] in conventional solvents. Fluorescence signature of ANF in the RTILs is expected to be more sensitive to those "transient" domains which could not be distinguished by the C153 due to its relatively longer excited state lifetime (τ = 3–5 ns).[14] Excitation wavelengths dependent steady state emission behavior of C153 and ANF has been carried out in both ionic liquids. A representative plot which shows the excitation wavelength dependence of emission peak frequency and spectral width (fwhm of emission spectra) of both C153and ANF is provided in Figure 10. As can be seen from Figure 10, the emission peak frequency of (ν_m) for ANF shifts by 630 cm^{-1} upon changing the λ_{exc} from bluest end to the most red end of the considered wavelengths, whereas the fluorescence maximum of C153 shows a very small shift (140 cm^{-1}). A similar result has been found in case of pyrrolidinium IL except for shifts of the emission peak frequency for ANF, which is found to be 430 cm^{-1}. The λ_{exc} dependence of fluorescence spectral width shows usual trend of narrowing down of fwhm with increased solvation for both the probes (Figure 10, lower panel). Figure 10 also depicts that the extent of narrowing down of fluorescence spectral width is approximately 6 times as large as that for C153. These data are useful in a sense that they provide an idea about the lifetime of microscopic structures that induce heterogeneity in these ILs. We note that the observation of red shift of λ_{em} maximum of the dipolar molecules when excited at the long-wavelength edge of the first absorption band is known as "red-edge effect" (REE).[26] Samanta and his co-workers previously observed that the excitation-wavelength-dependent shift of the fluorescence maximum of ANF increases with the increase in viscosity of the ILs.[11d] The REE is not generally observed in conventional medium of low viscosity. The REE phenomenon in ILs has been explained by considering the existence of a distribution of energetically different solvated probes in the ground state and a slower rate of their excited-state relaxation processes.[11d] Even though the results obtained in the present study cannot pinpoint any

dx.doi.org/10.1021/jp3101199 | J. Phys. Chem. B 2013, 117, 636–647

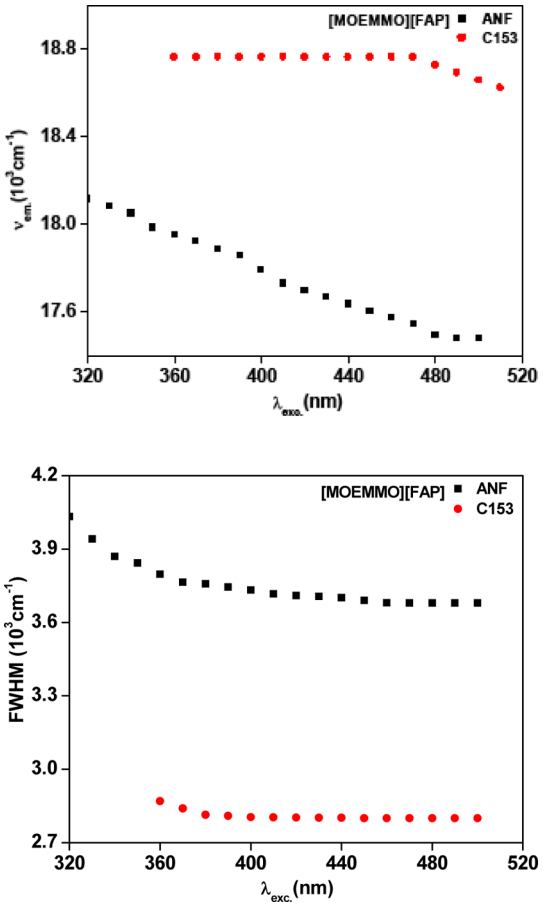

Figure 10. Excitation wavelength dependence (λ_{exc}) of emission peak frequency (ν_{em}) for ANF and C153 (upper panel) and full widths at half-maximum (fwhm) of emission spectra of the two solutes in [MOEMMO][FAP] (lower panel).

domain size or the length scale over which medium particles are correlated, they do provide evidence in favor of the spatial heterogeneity that exists in these RTILs. In other words, the observation reflects that high viscosity of the ionic liquid is complementary to microheterogeneity of the medium.

3.4. Rotational Dynamics of C153. To get further insight into the viscosity−diffusion decoupling, we have performed fluorescence anisotropy studies. Time resolved fluorescence anisotropy, $r(t)$, is determined by using the following equation

$$r(t) = \frac{GI_{VV}(t) - I_{VH}(t)}{GI_{VV}(t) + 2I_{VH}(t)} \text{ where } G = \frac{\sum I_{HH}(t)}{\sum I_{HV}(t)} \qquad (11)$$

where G is the instrument correction factor for detector sensitivity to the polarization direction of the emission. The G factor for our TCSPC setup is ∼0.7 at the wavelength of detection. $I_{HH}(t)$ and $I_{HV}(t)$ are the intensity of fluorescence decays when the excitation and the emission polarizer are polarized at horizontal−horizontal and horizontal−vertical alignment, respectively. Again, $I_{VV}(t)$ and $I_{VH}(t)$ are the intensity of fluorescence decays when excitation and emission polarizer are polarized at vertical−vertical and vertical−horizontal alignment, respectively. The anisotropy results at different λ_{exc} are collected in Table 7, and the anisotropy decay curves for C153 in neat RTILs at λ_{exc} = 405 nm are shown in Figure 11. The initial anisotropies, r_o, are found to vary from

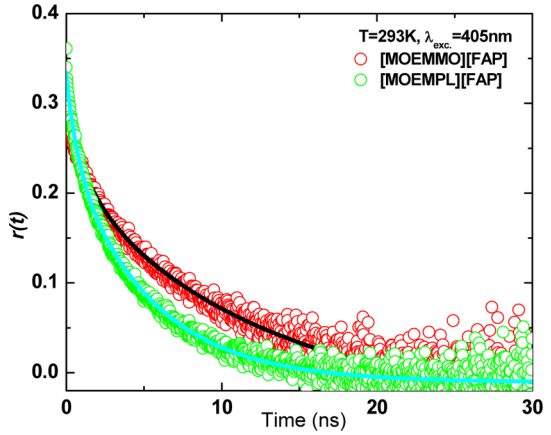

Figure 11. Time resolved fluorescence anisotropy decay (TRFAD) for C153 in [MOEMMO][FAP] and [MOEMPL][FAP] at 293 K. Solid lines in the same figure represent the biexponential fit to the data points. Data representations are clearly explained inside the panels. Notice that the anisotropy decays become slower in the case of [MOEMMO][FAP] due to the high viscosity.

0.31 to 0.36 for C153 in [MOEMPL][FAP] and [MOEMMO]-[FAP], respectively. The anisotropy decay profiles were fitted by both biexponential and single exponential functions as a function time. It was found that biexponential fits are marginally better than the single-exponential fits, and average rotational correlation times, $\langle\tau_{rot}\rangle$, obtained from the biexponential fits, were found to be almost similar to those obtained from the single-exponential fits. The uncertainties on $\langle\tau_{rot}\rangle$ values are usually in the range 2−5%, in [MOEMPL]-[FAP] for all temperatures except [MOEMMO][FAP] where the error is about 10% at low temperature because the recovered reorientation time is higher than the fluorescence lifetime. The uncertainties on the measured viscosities (η) are about 5%.

Interestingly, rotational relaxation data (see Table 7) reveal that the average rotational time increases only 2 times, whereas

Table 7. Reorientation Times of C153 in [MOEMMO][FAP] and [MOEMPL][FAP] at Different Excitation Wavelengths and at 293 K

system	viscosity (cP)	λ_{exc} (nm)[a]	a_1	τ_1 (ns)	a_2	τ_2 (ns)	$\langle\tau_{rot}\rangle$ (ns)[b]
MOEMPLFAP	128	375	0.27	1.04	0.72	6.75	5.88
		405	0.20	0.94	0.80	8.26	6.80
		445	0.13	2.34	0.87	6.34	5.82
MOEMMOFAP	1004	375	0.20	1.62	0.80	13.69	11.28
		405	0.26	2.42	0.74	15.70	12.25
		445	0.17	0.48	0.83	15.68	13.10

[a]Excitation wavelength. [b]Average rotational time.

dx.doi.org/10.1021/jp3101199 | J. Phys. Chem. B 2013, 117, 636−647

Table 8. Reorientation Times of C153 in [MOEMMO][FAP] and [MOEMPL][FAP] as a Function of Temperature at λ_{ex} = 405 nm

system	temp (K)	viscosity (cP)	a_1	τ_1 (ns)	a_2	τ_2 (ns)	$\langle\tau_{rot}\rangle$ (ns)[a]
MOEMPLFAP	293	128	0.20	0.94	0.80	8.26	6.80
	298	98	0.19	1.50	0.81	5.57	4.80
	303	75	0.23	1.08	0.77	4.27	3.54
	308	57	0.26	0.55	0.74	3.21	2.52
	313	46	0.24	0.54	0.76	2.61	2.11
MOEMMOFAP	293	1004	0.26	2.42	0.74	15.70	12.25
	298	657	0.25	2.28	0.75	14.30	11.29
	303	438	0.25	2.21	0.75	12.99	10.27
	308	301	0.21	1.27	0.79	11.16	9.08
	313	216	0.24	1.67	0.76	9.33	7.49
	318	154	0.18	0.81	0.82	7.45	6.25
	323	114	0.21	0.62	0.79	5.66	4.60
	328	85	0.23	0.93	0.77	5.02	4.08
	333	69	0.21	0.83	0.79	3.90	3.25

[a]Average rotational time.

the viscosity increases almost 8 times upon changing the medium from [MOEMPL][FAP] to [MOEMMO][FAP]. This observation clearly indicates that the rotational motion of C153 is not becoming as slow as is expected in relatively more viscous [MOEMMO][FAP]. Quite interestingly, rotational relaxation data (Table 7) also reveal that rotation at higher excitation wavelength (λ_{exc}) is slower for the more viscous IL. In this regard, we would like to recall the earlier observation with regard to solvation relaxation, where solvation time at higher λ_{exc} is also found to be slower for the more viscous IL (Table 4). The said observation is interesting. However, at this stage, we are unable to find out the exact origin of this behavior on the basis of the present data. Further work such as computer simulation studies is required to address this issue.

To have a better understanding of the rotational diffusion of C153, we have carried out rotational diffusion study of this particular probe in these two RTILs as a function of temperatures at 405 nm excitation wavelength. We have also analyzed the experimentally measured reorientation time with the help of the most popularly known Stokes–Einstein–Debye (SED) hydrodynamic theory. The anisotropy results of C153 at different temperature in these medium are collected in Table 8.

According to Stokes–Einstein–Debye theory, the rotational motion of a medium sized solute molecule in a solvent continuum is assumed to occur by small step diffusion, and its reorientation time is related to the bulk viscosity of the solvent and temperature by the following equation

$$\tau_r^{SED} = \frac{\eta V f C}{kT} \tag{12}$$

In the above relation, k is the Boltzmann constant, and T is absolute temperature. V is the van der Waals volume of the solute molecule, and C is the boundary condition parameter, which expresses the measure of coupling between the solute and the solvent. The two extreme boundary conditions are stick and slip according to SED hydrodynamic theory.[27] When the rotating solute molecule is bigger in size than solvent molecule, C is unity and it represents the stick boundary condition. In the case of a comparable or smaller solute molecule than the solvent, C is less than unity. Again, f is the shape factor which accounts for the nonspherical shapes of the solute molecules. The shapes of the solute molecules are usually incorporated into the SED theory by considering them as either symmetric or asymmetric ellipsoids. For nonspherical molecules, f is greater than unity, and the magnitude of the deviation from unity in the value of f describes the degree of nonspherical nature of the rotating solute molecule. For the calculation of slip boundary condition (C_{slip}), C153 has been treated as asymmetric ellipsoid, and the reorientation time was calculated. For calculation of C_{slip}, we have used the probe properties which are available in literature.[5b] Details of the calculation have been described in our earlier publications.[10e] The van der Waals volume, shape factor, and calculated slip boundary condition parameter for C153 are 243 Å^3, 1.5, and 0.18, respectively.[5b,10e] The slip and stick boundary conditions, which have been calculated with the help of SED hydrodynamic theory, are shown in Figure 12 with experimentally measured reorientation time of C153 in [MOEMPL][FAP] and [MOEMMO][FAP] RTILs, respectively. Estimated rotational coupling constant (C_{obs}) values are found to be similar to the conventional solvents for both ILs.[28]

From Figure 12, it is noticeable that the rotational diffusions of C153 in [MOEMPL][FAP] are in between stick and slip boundaries. However, at lower temperature, in highly viscous [MOEMMO][FAP] the rotational diffusion of C153 significantly departs from SED prediction (Figure 12). The departure from the SED theory predictions is quantified as $\tau_r \propto (\eta/T)^p$, with a p value 1.10 and 0.48 for [MOEMPL][FAP] and [MOEMMO][FAP] RTILs, respectively.

$$\text{C153 in [MOEMMO][FAP]} \log(\langle\tau_r\rangle) = 0.90 + 0.48 \log(\eta/T)\ (N = 9,\ R = 0.97224) \tag{13}$$

$$\text{C153 in[MOEMPL][FAP]} \log(\langle\tau_r\rangle) = 1.21 + 1.10 \log(\eta/T)\ (N = 5,\ R = 0.99799) \tag{14}$$

The observed higher degree of nonlinear behavior for the more viscous ionic liquid, [MOEMMO][FAP], is attributed to the pronounced heterogeneity of the medium.[12d] These seem to be interesting in a sense that earlier rotational dynamics studies showed better linear correlation with viscosity of the medium.[24] Figure 13 showed the deviation of present observation than the earlier report. In this context, it should be mentioned that a similar nonlinear response of average rotation relaxation time with viscosity has also been observed

dx.doi.org/10.1021/jp3101199 | J. Phys. Chem. B 2013, 117, 636–647

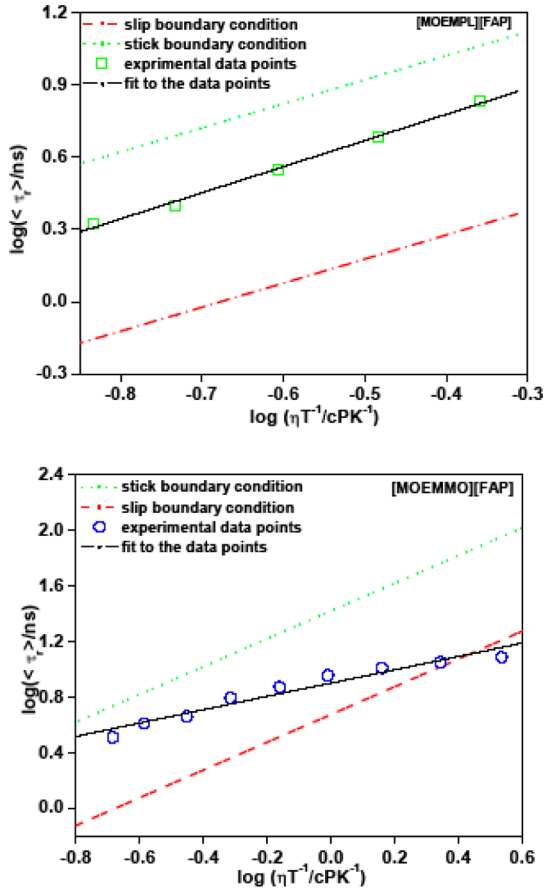

Figure 12. log–log plots of rotational relaxation time of C153 vs η/T in RTILs with slip and stick boundary condition parameters.

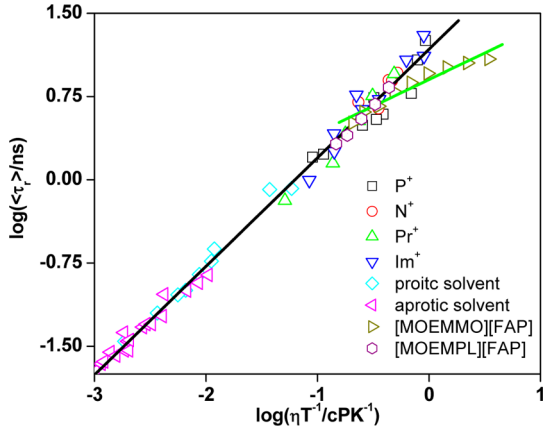

Figure 13. log–log plots of rotational relaxation time of C153 vs η/T in different RTILs. P^+, N^+ Pr^+, Im^+ denoted the phosphonium, ammonium, pyrrolidinium, and imidazolium cation containing RTILs which experimental data are taken from ref 24 . Experimental data for protic and aprotic solvent are taken from ref 28.

very recently by Samanta and his co-workers with morpholinium-based ILs, and they explained the observation on the basis of heterogeneity of the medium.[4i] Larger viscosity in an inhomogeneous medium is known to introduce larger decoupling.[25a] This arises due to the non-Brownian movement such as large angle jumps[29] and the retention of inertia driven motion even much after the onset of the typical diffusion time scale.[30] This alternative dynamic mode significantly reduces the frictional resistance against the diffusing particle arising from the macroscopic viscosity and thus strongly promotes departure from the conventional hydrodynamic description. It is pertinent to mention here that the results obtained from reactive and nonreactive dynamics studies in ionic liquids,[11g,i,n] and recent measurements in molecular liquids,[31] where ∼2 nm structural inhomogeneity in an otherwise homogeneous liquid in isothermal condition have been introduced, demonstrate that both the static and dynamic heterogeneities may contribute to probe rotation and medium viscosity. Moreover, the recent work by Biswas and co-workers also explains viscosity–diffusion phenomena in eutectic melts by invoking both static and dynamic heterogeneity.[12d] In this context, we would like to mention that solute and solvation relaxation experiments on eutectic melts[12d] and supercooled liquids[23] showed a higher p value for rotation than solvation. However, in the present case the observation of the larger value of fraction (p) for solvation than for rotation is interesting. We are not sure about the possible origin of this behavior at this stage. In this regard, it may be mentioned that the presence of fluorine atoms sometime causes anomalous photophysical behavior.[32,33] Since the present ionic liquids also contain a fluorine atom in their anionic constituents, the present observation may be linked to those studies. However, further studies are required to rationalize the observed behavior.

Keeping in mind the latest literature findings and the observation of the higher shift in the excitation wavelength dependent fluorescence both in steady state and time-resolved measurements, this indicates that static and dynamic heterogeneity of the medium may contribute to the fractional dependence of average rotational time on viscosity in highly viscous ionic liquid.

CONCLUSION

Time-resolved fluorescence Stokes shift and anisotropy measurements of coumarin 153 are investigated in two hydrophobic ionic liquids (ILs), [MOEMMO][FAP] and [MOEMPL][FAP]. Viscosity of the [MOEMMO][FAP] is measured to be 8 times higher than that of [MOEMPL][FAP]. In the case of a more viscous ionic liquid, the solvation and rotational relaxation times are not found to be as slow as are expected from the bulk viscosity value. The breakdown of both Stokes–Einstein (SE) and Stokes–Einstein–Debye (SED) relationships has been observed. The observation indicates a significant viscosity–diffusion decoupling during solvation and rotational relaxation of C153 in higher viscous IL. The decoupling is also analyzed through fractional viscosity dependence of the measured average solvation $\langle\tau_s\rangle$ and rotation $\langle\tau_r\rangle$ times: $\langle\tau_x\rangle \propto (\eta/T)^p$ (x is solvation or rotation, p is the exponent, and T is the temperature). The excitation wavelength dependent fluorescence studies have been carried out to correlate the experimental findings with the medium heterogeneity. The observation seems to suggest that both static and dynamic heterogeneity may play an important role for the observed viscosity–diffusion (d–η) decoupling in highly viscous ionic liquid. However, more studies comprising both theoretical and experimental investigations are required to throw more light on this aspect.

ASSOCIATED CONTENT

Supporting Information

Additional table and figures. This material is available free of charge via the Internet at http://pubs.acs.org.

dx.doi.org/10.1021/jp3101199 | J. Phys. Chem. B 2013, 117, 636–647

AUTHOR INFORMATION

Corresponding Author

*E-mail: msarkar@niser.ac.in. Fax: +91-674-2304050. Phone: +91-674-2304037.

Notes

The authors declare no competing financial interest.

ACKNOWLEDGMENTS

The authors thank anonymous reviewers for constructive criticism and insightful comments. The comments have been very useful in improving the quality of the manuscript. This work has been supported by the Department of Science and Technology (DST), Government of India. S.K.D. thanks the Council of Scientific and Industrial Research (CSIR), New Delhi, for awarding a fellowship. P.K.S. thanks the National Institute of Science Education and Research (NISER), Bhubaneswar, for the fellowship awarded to him.

REFERENCES

(1) Rogers, R. D.; Seddon, K. R. *Science* **2003**, *302*, 792−793.

(2) (a) Welton, T. *Chem. Rev.* **1999**, *99*, 2071−2084. (b) Sheldon, R. *Chem. Commun.* **2001**, 2399−2407. (c) Hayashi, S.; Ozawa, R.; Hamaguchi, H. *Chem. Lett.* **2004**, *33*, 1590−1591. (d) Dupont, J.; de Suza, R. F.; Suarez, P. A. Z. *Chem. Rev.* **2002**, *102*, 3667−3692. (e) Wasserscheid, P.; Keim, W. *Angew. Chem., Int. Ed.* **2000**, *39*, 3772−3789. (f) Hough, W. L.; Rogers, R. D. *Bull. Chem. Soc. Jpn.* **2007**, *80*, 2262−2269. (g) Plechkova, N. V.; Seddon, K. R. *Chem. Soc. Rev.* **2008**, *37*, 123−150. (h) Rogers, R. D.; Voth, G. A. *Acc. Chem. Res.* **2007**, *40*, 1077−1078. (i) Chiappe, C.; Pieraccini, D. *J. Phys. Org. Chem.* **2005**, *18*, 275−297. (j) Weingartner, H. *Angew. Chem., Int. Ed.* **2008**, *47*, 654−670. (k) Chiappe, C.; Konig, B.; Impareto, G. *Eur. J. Org. Chem.* **2007**, 1049−1058. (l) Rantwijk, F. V.; Sheldon, R. *Chem. Rev.* **2007**, *107*, 2757−2785.

(3) Jimenez, R.; Fleming, G. R.; Kumar, P. V.; Maroncelli, M. *Nature* **1994**, *369*, 471−473.

(4) (a) Karmakar, R.; Samanta, A. *J. Phys. Chem. A* **2002**, *106*, 4447−4452. (b) Karamkar, R.; Samanta, A. *J. Phys. Chem. A* **2002**, *106*, 6670−6675. (c) Karmakar, R.; Samanta, A. *J. Phys. Chem. A* **2003**, *107*, 7340−7346. (d) Mandal, P. K.; Samanta, A. *J. Phys. Chem. B* **2005**, *109*, 15172−15177. (e) Mandal, P. K.; Saha, S.; Karmakar, R.; Samanta, A. *Curr. Sci.* **2006**, *90*, 301−310. (f) Samanta, A. *J. Phys. Chem. B* **2006**, *110*, 13704−13716. (g) Paul, A.; Samanta, A. *J. Phys. Chem. B* **2007**, *111*, 4724−4731. (h) Samanta, A. *J. Phys. Chem. Lett.* **2010**, *1*, 1557−1562. (i) Khara, D. C.; Samanta, A. *J. Phys. Chem. B* **2012**, *116*, 13430−13438.

(5) (a) Ingram, J. A.; Moog, R. S.; Ito, N.; Biswas, R.; Maroncelli, M. *J. Phys. Chem. B* **2003**, *107*, 5926−5932. (b) Ito, N.; Arzhantsev, S.; Maroncelli, M. *Chem. Phys. Lett.* **2004**, *396*, 83−91. (c) Arzhantsev, S.; Jin, H.; Baker, G. A.; Maroncelli, M. *J. Phys. Chem. B* **2007**, *111*, 4978−4989. (d) Jin, H.; Li, X.; Maroncelli, M. *J. Phys. Chem. B* **2007**, *111*, 13473−13478. (e) Jin, H.; Baker, G. A.; Arzhantsev, S.; Dong, J.; Maroncelli, M. *J. Phys. Chem. B* **2007**, *111*, 7291−7302. (f) Jin, H.; O'Hare, B.; Dong, J.; Arzhantsev, S.; Baker, G. A.; Wishart, J. F.; Benesi, A. J.; Maroncelli, M. *J. Phys. Chem. B* **2008**, *112*, 81−92. (g) Roy, D.; Patel, N.; Conte, S.; Maroncelli, M. *J. Phys. Chem. B* **2010**, *114*, 8410−8424. (h) Roy, D.; Maroncelli, M. *J. Phys. Chem. B* **2010**, *114*, 12629−12631.

(6) (a) Chakrabarty, D.; Chakraborty, A.; Seth, D.; Sarkar, N. *J. Phys. Chem. A* **2005**, *109*, 1764−1769. (b) Chakraborty, A.; Seth, D.; Chakrabarty, D.; Setua, P.; Sarkar, N. *J. Phys. Chem. A* **2005**, *109*, 11110−11116. (c) Chakrabarty, D.; Hazra, P.; Chakraborty, A.; Seth, D.; Sarkar, N. *Chem. Phys. Lett.* **2003**, *381*, 697−704. (d) Seth, D.; Sarkar, S.; Sarkar, N. *J. Phys. Chem. B* **2008**, *112*, 2629−2636. (e) Pramanik, R.; Rao, V. G.; Sarkar, S.; Ghatak, C.; Setua, P.; Sarkar, N. *J. Phys. Chem. B* **2009**, *113*, 8626−8634. (f) Sarkar, S.; Pramanik, R.; Ghatak, C.; Setua, P.; Sarkar, N. *J. Phys. Chem. B* **2010**, *114*, 2779−2789.

(7) (a) Chowdhury, P. K.; Halder, M.; Sanders, L.; Calhoun, T.; Anderson, J. L.; Armstrong, W. D.; Song, X.; Petrich, J. W. *J. Phys. Chem. B* **2004**, *108*, 10245−10255. (b) Carlson, P. J.; Bose, S.; Armstrong, D. W.; Hawkins, T.; Gordon, M. S.; Petrich, J. W. *J. Phys. Chem. B* **2012**, *116*, 503−512.

(8) (a) Kashyap, H. K.; Biswas, R. *J. Phys. Chem. B* **2008**, *112*, 12431−12438. (b) Kashyap, H. K.; Biswas, R. *J. Phys. Chem. B* **2010**, *114*, 254−268. (c) Kashyap, H. K.; Biswas, R. *J. Phys. Chem. B* **2010**, *114*, 16811−16823. (d) Kashyap, H. K.; Biswas, R. *Indian J. Chem.* **2010**, *49A*, 685−694. (e) Daschakraborty, S.; Biswas, R. *J. Phys. Chem. B* **2011**, *115*, 4011−4024. (f) Daschakraborty, S.; Biswas, R. *Chem. Phys. Lett.* **2011**, *510*, 202−207.

(9) (a) Das, S. K.; Sarkar, M. *Chem. Phys. Lett.* **2011**, *515*, 23−28. (b) Das, S. K.; Sarkar, M. *J. Mol. Liq.* **2012**, *165*, 38−43. (c) Das, S. K.; Sarkar, M. *J. Lumin.* **2012**, *132*, 368−374. (d) Das, S. K.; Sarkar, M. *ChemPhysChem* **2012**, *13*, 2761−2768.

(10) (a) Khara, D. C.; Samanta, A. *Phys. Chem. Chem. Phys.* **2010**, *12*, 7671−7677. (b) Dutt, G. B. *J. Phys. Chem. B* **2010**, *114*, 8971−8977. (c) Karve, L.; Dutt, G. B. *J. Phys. Chem. B* **2011**, *115*, 725−729. (d) Fruchey, K.; Fayer, M. D. *J. Phys. Chem. B* **2010**, *114*, 2840−2845. (e) Das, S. K.; Sarkar, M. *J. Phys. Chem. B* **2012**, *116*, 194−202.

(11) (a) Wang, Y.; Voth, G. A. *J. Am. Chem. Soc.* **2005**, *127*, 12192−12193. (b) Lopes, J. N. A. C.; Padua, A. A. H. *J. Phys. Chem. B* **2006**, *110*, 3330−3335. (c) Xiao, D.; Rajian, J. R.; Cady, A.; Li, S.; Bartsch, R. A.; Quitevis, E. L. *J. Phys. Chem. B* **2007**, *111*, 4669−4677. (d) Mandal, P. K.; Sarkar, M.; Samanta, A. *J. Phys. Chem. A* **2004**, *108*, 9048−9053. (e) Mandal, P. K.; Paul, A.; Samanta, A. *J. Photochem. Photobiol.* **2006**, *182*, 113−120. (f) Paul, A.; Samanta, A. *J. Phys. Chem. B* **2007**, *111*, 1957−1962. (g) Santhosh, K.; Banerjee, S.; Rangaraj, N.; Samanta, A. *J. Phys. Chem. B* **2010**, *114*, 1967−1974. (h) Hu, Z.; Margulis, C. *J. Proc. Natl. Acad. Sci. U.S.A.* **2006**, *103*, 831−836. (i) Kobrak, M. N. *J. Chem. Phys.* **2006**, *125*, 064502. (j) Shim, Y.; Jeong, D.; Manjari, S.; Choi, M. Y.; Kim, H. *Acc. Chem. Res.* **2007**, *40*, 1130−1137. (k) Jin, H.; Li, X.; Maroncelli, M. *J. Phys. Chem. B* **2007**, *111*, 13473−13478. (l) Shirota, H.; Wishart, J. F.; Castner, E. W., Jr. *J. Phys. Chem. B* **2007**, *111*, 4819−4829. (m) Adhikari, A.; Sahu, K.; Dey, S.; Ghosh, S.; Mandal, U.; Bhattacharyya, K. *J. Phys. Chem. B* **2007**, *111*, 12809−12816. (n) Kimura, Y.; Fukuda, M.; Suda, K.; Terazima, M. *J. Phys. Chem. B* **2010**, *114*, 11847−11858.

(12) (a) Guchhait, B.; Gazi, H. A. R.; Kashyap, H. K.; Biswas, R. *J. Phys. Chem. B* **2010**, *114*, 5066−5081. (b) Gazi, H. A. R.; Guchhait, B.; Daschakraborty, S.; Biswas, R. *Chem. Phys. Lett.* **2011**, *501*, 358−363. (c) Pal, T.; Biswas, R. *Chem. Phys. Lett.* **2011**, *517*, 180−185. (d) Guchhait, B.; Daschakraborty, S.; Biswas, R. *J. Chem. Phys.* **2012**, *136*, 11847.

(13) Yao, C.; Pitner, W. R.; Anderson, J. L. *Anal. Chem.* **2009**, *81*, 5054−5063.

(14) Horng, M. -L.; Gardecki, J. A.; Papazyan, A.; Maroncelli, M. *J. Phys. Chem.* **1995**, *99*, 17311−17337.

(15) Maroncelli, M.; Fleming, G. R. *J. Chem. Phys.* **1987**, *86*, 6221.

(16) Dewar, M. J. S.; Zoesisch, E. G.; Healy, E. F.; Stewart, J. J. P. *J. Am. Chem. Soc.* **1985**, *102*, 3902−3905.

(17) Frisch, M. J.; Trucks, G. W.; Schlegel, H. B.; Scuseria, G. E.; Robb, M. A.; Cheeseman, J. R.; Zakrzewski, V. G.; Montgomery, J. A., Jr.; Stratmann, R. E.; Burant, J. C.; et al. *Gaussian 03, RevisionC.02*; Gaussian, Inc.: Wallingford, CT, 2004.

(18) Ziyada, A. K.; Wilfred, C. D.; Bustam, M. A.; Man, Z.; Murugesan, T. *J. Chem. Eng. Data* **2010**, *55*, 3886−3890.

(19) Muhammad, N.; Man, Z. B.; Bustam, M. A.; Mutalib, M. I. A.; Wilfred, C. D.; Rafiq, S. *J. Chem. Eng. Data* **2011**, *56*, 3157−3162.

(20) Muhammad, N.; Man, Z.; Ziyada, A. K.; Bustam, M. A.; Mutalib, M. I. A.; Wilfred, C. D.; Rafiq, S.; Tan, I. M. *J. Chem. Eng. Data* **2012**, *57*, 737−743.

(21) Gu, Z.; Brennecke, J. F. *J. Chem. Eng. Data* **2002**, *47*, 339−345.

(22) Taib, M. M.; Ziyada, A. K.; Wilfred, C. D.; Murugesan. *J. Mol. Liq.* **2011**, *158*, 101−104.

(23) Fee, R. S.; Maroncelli, M. *Chem. Phys.* **1994**, *183*, 235−247.

(24) Jin, H.; Baker, G. A.; Arzhantsev, S.; Dong, J.; Maroncelli, M. *J. Phys. Chem. B* **2007**, *111*, 7291−7302.
(25) (a) Ediger, M. D. *Annu. Rev. Phys. Chem.* **2000**, *51*, 99−128. (b) Sillescu, H. *J. Non-Cryst. Solids* **1999**, *243*, 81−108. (c) Ediger, M. D.; Angell, C. A.; Nagel, S. R. *J. Phys. Chem.* **1996**, *100*, 13200−13212. (d) Moynihan, C. T. *J. Phys. Chem.* **1966**, *70*, 3399−3406. (e) Angell, C. A. *J. Chem. Phys.* **1967**, *46*, 4673. (f) Chakrabarti, D.; Bagchi, B. *Phys. Rev. Lett.* **2006**, *96*, 187801.
(26) (a) Valeur, B.; Weber, G. *Chem. Phys. Lett.* **1977**, *45*, 140−144. (b) Weber, G.; Shinitzky, M. *Proc. Natl. Acad. Sci. U.S.A.* **1970**, *65*, 823−830.
(27) Hu, C. M.; Zwanzig, R. *J. Chem. Phys.* **1974**, *60*, 4354.
(28) Horng, M.-L.; Gardecki, J.; Maroncelli, M. *J. Phys. Chem. A* **1997**, *101*, 1030−1047.
(29) Shlesinger, M. F.; Zaslavsky, G. M.; Klafter, J. *Nature* **1993**, *363*, 31−37.
(30) (a) Habasaki, J.; Ngai, K. L. *J. Chem. Phys.* **2008**, *129*, 194501. (b) Hu, Z.; Huang, X.; Annapureddy, H. V. R.; Margulis, C. J. *J. Phys. Chem. B* **2008**, *112*, 7837−7849.
(31) Ueno, K.; Angell, C. A. *J. Phys. Chem. B* **2011**, *115*, 13994−13999.
(32) Kwon, O.-H.; Yoo, T. H.; Othon, C. M.; Deventer, J. A. V.; Tirrel, D. A.; Zewail, A. H. *J. Proc. Natl. Acad. Sci. U.S.A.* **2010**, *107*, 17101−17106.
(33) Li, M.; Jiang, M.; Zhang, Y.-X.; Fang, Q. *Macromolecules* **1997**, *30*, 470−478.